Molecular Crystals and Liquid Crystals

Publication details, including instructions for authors and subscription information:
http://www.tandfonline.com/loi/gmcl20

Analysis of Ring Patterns in SmC* Liquid Crystals

E. J. Wigham [a] & I. W. Stewart [a]

[a] Department of Mathematics, University of Strathclyde, Livingstone Tower, Glasgow, UK

Version of record first published: 31 Aug 2006

To cite this article: E. J. Wigham & I. W. Stewart (2005): Analysis of Ring Patterns in SmC* Liquid Crystals, Molecular Crystals and Liquid Crystals, 436:1, 1/[955]-15/[969]

To link to this article: http://dx.doi.org/10.1080/15421400590955532

Mol. Cryst. Liq. Cryst., Vol. 436, pp. 1/[955]–15/[969], 2005

ISSN: 1542-1406 print/1563-5287 online
DOI: 10.1080/15421400590955532

Taylor & Francis
Taylor & Francis Group

Analysis of Ring Patterns in SmC* Liquid Crystals

E. J. Wigham
I. W. Stewart
Department of Mathematics, University of Strathclyde, Livingstone Tower, Glasgow, UK

It has been seen experimentally that ring patterns occur when planar aligned samples of SmC are subjected to a rotating in-plane electric field [4,7,12]. We shall model this problem mathematically by approximating the ring patterns and considering a circular domain embedded within a rectangular sample. The ring patterns will be modelled by travelling wave solutions. We shall then investigate the stability of these travelling wave solutions via a linearised perturbation, a Hardy-type inequality and an isoperimetric minimisation problem. This allows a calculation of the lowest eigenvalue which we use to determine the response time of perturbations to the travelling wave solution.*

Keywords: ring patterns; smectic C liquid crystals; stability

INTRODUCTION

The alignment of the director in SmC* liquid crystals is known to be influenced by electric or magnetic fields. It has been seen experimentally by Dascalu *et al.* [4], Hauck, Koswig and Labes [7], and Link *et al.* [12] that ring patterns occur when planar aligned samples of SmC* are subjected to a rotating in-plane electric field. A theoretical investigation of ring patterns has been made by Kilian, Koswig and Sonnet [9] based upon Landau theory and approximations using the Goldstone mode. In their analysis, Kilian *et al.* have neglected any dielectric contribution and have made an approximation which disregards a radially-dependent term.

The work presented here will incorporate the dielectric contribution and all radially-dependent terms. The governing dynamic equation for

Address correspondence to E. J. Wigham, Department of Mathematics, University of Strathclyde, Livingstone Tower, 26 Richmond Street, Glasgow G1 1XH, UK. E-mail: ta.ewig@maths.strath.ac.uk

a sample of SmC*, derived from the theory introduced by Leslie, Stewart and Nakagawa [11,15], will be obtained for an analogue of the well-known experiment for nematics reported by Zwetkoff [16].

GOVERNING DYNAMIC EQUATION

In 1939 Zwetkoff originally set up an experiment in nematics under a rotating magnetic field to determine the rotational viscosity γ_1 [16]. Here we shall adapt this experiment and its calculations for a SmC* sample to obtain our governing dynamic equation. It can be considered applicable to both cylindrical and planar aligned samples.

The set-up of our experiment is as follows. Firstly, we have a thin rectangular sample of SmC* liquid crystal under the influence of an electric field, **E**, acting in a horizontal plane. We shall approximate the domain of investigation within this rectangular cell by a large cylindrical region of radius R and cell depth d. We then rotate our field at a constant angular velocity ω about the vertical axis as shown in Figure 1. It may be easier to rotate the sample in a fixed field, but the situation is equivalent when the fluid velocity **v** is neglected, as it will be here.

We may introduce **a**, **c**, **E** and **P** as

$$\mathbf{a} = (0, 0, 1), \quad \mathbf{c} = (\cos\phi, \sin\phi, 0), \tag{1}$$

$$\mathbf{E} = E_0(\cos\omega t, \sin\omega t, 0), \quad \mathbf{P} = P_0(-\sin\phi, \cos\phi, 0), \tag{2}$$

where E_0 is the magnitude of the electric field, and the spontaneous polarisation **P** is taken to be positive with $P_0 > 0$, defined in the usual sense for such materials [15].

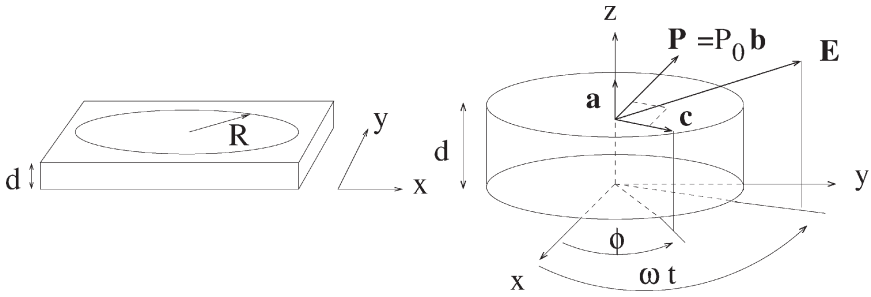

FIGURE 1 The left figure is the set-up of the experiment within a rectangular cell containing a sample of SmC* liquid crystal. The right figure displays a large cylindrical region approximating the domain of investigation within the rectangular cell radius R and cell depth d.

For incompressible SmC* the general governing dynamic equations, in the absence of any generalised external body forces, are [11,15]

$$\rho \dot{v}_i = \rho F_i - \tilde{p}_{,i} + \tilde{g}^a_k a_{k,i} + \tilde{g}^c_k c_{k,i} + \tilde{t}_{ij,j}, \tag{3}$$

$$\left(\frac{\partial w}{\partial a_{i,j}}\right)_{,j} - \frac{\partial w}{\partial a_i} + \tilde{g}^a_i + \gamma a_i + \mu c_i + \epsilon_{ijk}\beta_{k,j} = 0, \tag{4}$$

$$\left(\frac{\partial w}{\partial c_{i,j}}\right)_{,j} - \frac{\partial w}{\partial c_i} + \tilde{g}^c_i + \tau c_i + \mu a_i = 0, \tag{5}$$

where $\mathbf{v}$ is the velocity, ρF_i is the external body force per unit volume, p is the pressure, $\mathbf{w}$ is the total energy density for SmC*, $\tilde{g}^a_i$ and $\tilde{g}^c_i$ are dynamic contributions and $\tilde{t}_{ij}$ is the viscous stress. A superposed dot represents the usual material time derivative. The scalar functions γ, μ and τ, and the vector function β, are lagrange multipliers which arise from the usual smectic theory constraints that $\mathbf{a}$ and $\mathbf{c}$ are mutually orthogonal unit vectors and $\nabla \times \mathbf{a} = \mathbf{0}$, this latter constraint being valid when there are no dislocations in the sample [14]. In this present problem, w can be calculated from the general forms for the elastic and electric energy densities to find [15, pp. 310–311]

$$\begin{aligned} w = {} & \frac{1}{2}B_1(\cos^2\phi\phi_x^2 + \sin^2\phi\phi_y^2 + 2\sin\phi\cos\phi\phi_x\phi_y) \\ & + \frac{1}{2}B_2(\sin^2\phi\phi_x^2 + \cos^2\phi\phi_y^2 - 2\sin\phi\cos\phi\phi_x\phi_y) \\ & + \frac{1}{2}B_3 q^2 - \frac{1}{2}\epsilon_0\epsilon_a E_0^2\cos^2(\omega t - \phi)\sin^2\theta - P_0E_0\sin(\omega t - \phi), \end{aligned} \tag{6}$$

where B_1, B_2 and B_3 are elastic constants and q is a wave number, related to the pitch p of the inherent helical structure of the SmC* phase. The permittivity of free space is denoted by ϵ_0 while the (unitless) dielectric constant is denoted by ϵ_a.

We shall focus our attention on the behaviour at a relatively large radial distance: it is then feasible to ignore boundary effects and spatial gradients in the bulk. We may therefore set $\mathbf{v} = \mathbf{0}$ as an approximation and neglect gravity to find that Eq. (3) can be integrated to reveal that $\tilde{p}$ is a constant. To simplify matters further, the one-constant approximation $B_1 = B_2 \equiv B$ will be supposed. From Eqs. (4) and (5) we can explicitly find, or eliminate, the Lagrange multipliers γ, μ, τ and β by standard procedures [15, pp. 226–227]. Following such calculations, we find that the six equations expressed in (4) and (5)

reduce to the single dynamic equation

$$2\lambda_5 \frac{\partial \phi}{\partial t} = \frac{1}{2}\epsilon_0 \epsilon_a E_0^2 \sin^2\theta \sin\left(2(\omega t - \phi)\right) + P_0 E_0 \cos\left(\omega t - \phi\right) + B\nabla^2\phi,$$

where $\lambda_5 > 0$ is a rotational viscosity and ∇^2 represents the usual Laplacian operator. This equation can be recast into a form previously reported in [9, Eq. (17)] if we redefine ϕ by $\phi - \pi/2$, giving

$$\frac{\partial \phi}{\partial t} = \frac{P_0 E_0}{2\lambda_5}\sin\left(\omega t - \phi\right) - \frac{\varepsilon_0 \varepsilon_a}{4\lambda_5} E_0^2 \sin^2\theta \sin\left(2(\omega t - \phi)\right) + \frac{B}{2\lambda_5}\nabla^2\phi, \quad (7)$$

the key addition being the appearance of the dielectric term. It is the analysis of this equation that is our main concern.

RING PATTERN ANALYSIS

Since we are analysing ring patterns which are usually more or less cylindrical we shall change from cartesian to polar coordinates. It will be supposed that there is no dependence on the polar angle θ, which leads to the assumption that $\phi = \phi(r, t)$. Ring patterns emanating from the centre of a sample of SmC* have been seen experimentally by Dascalu *et al.* [4]. Motivated by these ring patterns, we choose a fixed relatively large radial distance $a > 0$ and approximate the 'width' of a typical ring as 5% of the radial distance between the midpoints of two adjacent rings. Specifically, we will look at a ring between $r = a$ and $r = (1.05)a$ where $a = 5 \times 10^{-4}$m [4] (see Fig. 2).

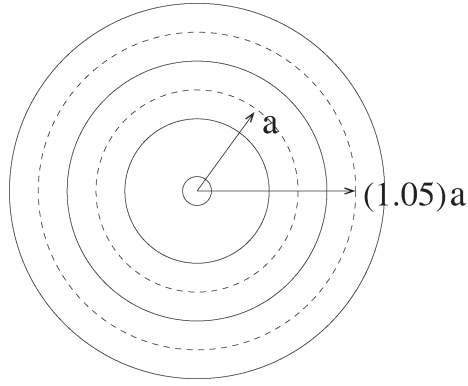

FIGURE 2 Schematic model of ring pattern.

In the polar coordinate system the governing Eq. (7) becomes

$$\frac{\partial \phi}{\partial t} = \frac{P_0 E_0}{2\lambda_5}\sin(\omega t - \phi) - \frac{\varepsilon_0 \varepsilon_a E_0^2 \sin^2\theta}{4\lambda_5}\sin(2(\omega t - \phi)) + \frac{B}{2\lambda_5}\left(\phi_{rr} + \frac{1}{r}\phi_r\right). \tag{8}$$

To simplify this equation further we choose to set $u = \omega t - \phi$, where u is our phase-lag angle, and rescale using

$$\hat{t} = \frac{\epsilon_0 \epsilon_a}{2\lambda_5} E_0^2 \sin^2\theta\, t, \qquad \hat{s} = \frac{1}{k}\ln\left(\frac{r}{a}\right), \qquad k^2 = 3.673 \times 10^{-9}, \tag{9}$$

where k^2 is a constant which approximates the coefficient of our spatial derivative over the range of one ring and applicable $\hat{s}$. We may then obtain the form of our dynamic equation to be

$$u_{\hat{t}} = f(u) + u_{\hat{s}\hat{s}}, \tag{10}$$

where

$$f(u) = \hat{\omega} + b\sin u + \sin u \cos u,\ b = \frac{-P_0}{\epsilon_0 \epsilon_a E_0 \sin^2\theta},\ \hat{\omega} = \frac{2\lambda_5}{\epsilon_0 \epsilon_a E_0^2 \sin^2\theta}\omega, \tag{11}$$

and b and $\hat{\omega}$ are dimensionless.

The governing dynamic Eq. (10) cannot be solved exactly when $\hat{\omega} \neq 0$ and so we approximate $f(u)$ to make the problem more tractable. By introducing an approximation we will lose our sinusoidal dependence which consequently means a loss in the modelling of multiple rings: however, the essential features of one single ring should persist if $f(u)$ is replaced by a reasonable nonlinear approximation which captures its sinusoidal behaviour.

Approximation by Orthonormal Polynomials

Since we cannot solve (10) explicitly we need to approximate $f(u)$ by the best fit cubic $g(u)$ via orthogonal polynomials. To ensure we have three real roots u_1, u_2, and u_3 of the function $f(u)$ we require to assume

$$0 \leq \omega \leq \omega_c \qquad \text{and} \qquad |b| \leq 1, \tag{12}$$

where ω_c is an upper limit on ω that can be found numerically: ω_c is the least value of ω for which $f(u)$ is non-negative for all u. Following

Hochstadt [8], it is know that the best fit cubic $g(u)$ in the space $L^2([a,b])$ is given by

$$g(u) = \sum_{k=0}^{3} \alpha_k \phi_k(u),$$

where α_k are constants determined by the relation

$$\alpha_k = \int_a^b f(u)\phi_k(u)du,$$

and $\{\phi_k(u)\}$ is an orthonormal set of polynomials where each of the ϕ_k has corresponding degree k. They are related to the Legendre polynomials through the identity

$$\phi_k(u) = \sqrt{\frac{2k+1}{2}} P_k(u). \tag{13}$$

Hence the cubic approximation may be stated explicitly as

$$g(u) = \hat{\omega} + \frac{12b}{\pi} + \frac{5}{\pi} - \frac{120b}{\pi^3} - \frac{105}{2\pi^3} + u\left(\frac{720b}{\pi^4} - \frac{45}{\pi^2} - \frac{60b}{\pi^2} + \frac{630}{\pi^4}\right) + u^2\left(-\frac{720b}{\pi^5} + \frac{105}{\pi^3} + \frac{60b}{\pi^3} - \frac{1575}{\pi^5}\right) + u^3\left(-\frac{70}{\pi^4} + \frac{1050}{\pi^6}\right). \tag{14}$$

The comparison between this best fit approximation $g(u)$ and the original function $f(u)$ may be seen in Figure 3. Equation (10) can now be approximated by

$$u_{\hat{t}} = g(u) + u_{\hat{s}\hat{s}}, \tag{15}$$

with the roots of $g(u)$ being found analytically following standard methods [1].

Soliton-Like Solution

With the explicit cubic roots, u_1, u_2 and u_3 in ascending order, of $g(u)$ we can solve our dynamical Eq. (15) exactly. For a travelling wave solution we set

$$\tau = \hat{s} - c\hat{t}, \tag{16}$$

which enables Eq. (15) to be rewritten as

$$cu_\tau + u_{\tau\tau} - (u-u_1)(u-u_2)(u-u_3) = 0. \tag{17}$$

From Lam and Prost [10] it is known that this equation has three soliton-like travelling wave solutions (TWS) given by

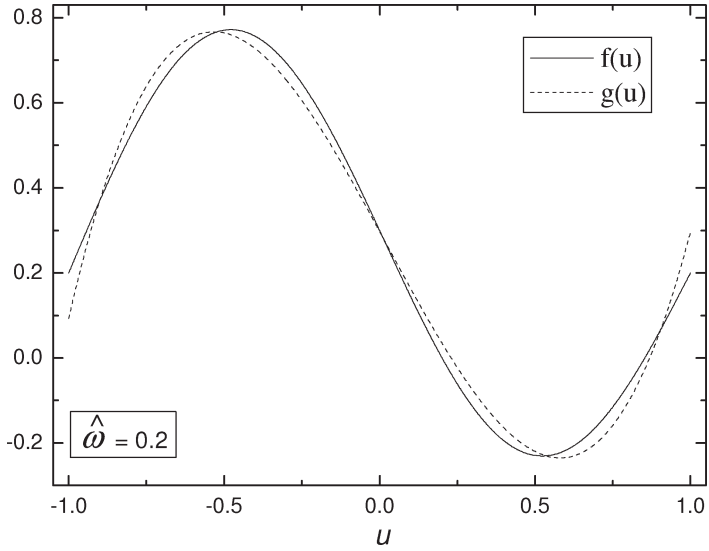

FIGURE 3 A typical qualitative comparison of the original sinusoidal $f(u)$ and the best fit cubic $g(u)$ when $\hat{\omega} = 0.2$ and $b = 0.1$.

$$u(\tau) = \frac{u_j - u_i}{(1 + \exp \bar{a}\tau)} + u_i, \qquad i \neq j, \tag{18}$$

where

$$\bar{a} = \frac{\varepsilon}{\sqrt{2}}(u_j - u_i), \quad c = \frac{\varepsilon}{\sqrt{2}}(u_j + u_i - 2u_k), \quad \varepsilon = \pm 1, \qquad i \neq j \neq k. \tag{19}$$

Our solutions travel between any two of the three roots i.e., $u_1 \to u_2$, $u_2 \to u_3$ or $u_3 \to u_1$. One particularly relevant soliton-like solution to our problem is

$$u(\tau) = \frac{u_3 - u_2}{(1 + \exp \bar{a}\tau)} + u_2, \tag{20}$$

where

$$u(\tau) \to u_2 \text{ as } \tau \to \infty, \qquad u(\tau) \to u_3 \text{ as } \tau \to -\infty, \tag{21}$$

where choosing $\epsilon = -1$, this representative soliton-like solution such as that depicted in Figure 4 where the reorientation of the angle in the original space and time coordinates, as shown, represents one 'ring' observed in an experiment. This ring is travelling in a soliton-like manner, as observed over various time steps.

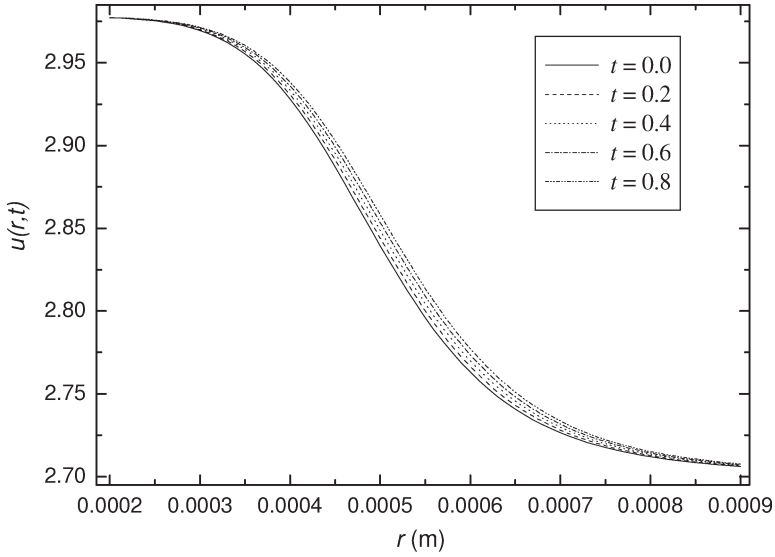

FIGURE 4 Qualitative plots of the soliton $u(r,t)$ at various time steps with $\hat{\omega} = 0.03$ and $b = 0.9$.

STABILITY ANALYSIS

Travelling Wave Solution Stability Analysis

Following Logan [13] we can perform a stability analysis for $-L \leq \tau \leq L$, for some $L > 0$, with the aim of gaining qualitative insight into the stability properties. Our governing Eq. (15) may be rearranged and written in a moving coordinate frame by considering $U(\tau,t) \equiv u(\hat{s},t)$ by changing the variables to

$$\hat{t} = \hat{t}, \qquad \tau = \hat{s} - c\hat{t}, \tag{22}$$

which yields

$$\begin{aligned} U_t - U_{\tau\tau} - cU_\tau = \hat{\omega} &+ \frac{12b}{\pi} + \frac{5}{\pi} - \frac{120b}{\pi^3} - \frac{105}{2\pi^3} \\ &+ U\left(\frac{720b}{\pi^4} - \frac{45}{\pi^2} - \frac{60b}{\pi^2} + \frac{630}{\pi^4}\right) \\ &+ U^2\left(-\frac{720b}{\pi^5} + \frac{105}{\pi^3} + \frac{60b}{\pi^3} - \frac{1575}{\pi^5}\right) \\ &+ U^3\left(-\frac{70}{\pi^4} + \frac{1050}{\pi^6}\right). \end{aligned} \tag{23}$$

We want to consider solutions of (23) of the form

$$U(\tau,t) = u(\tau) + V(\tau,t), \tag{24}$$

where V is a small perturbation to the travelling wave $u(\tau)$ given by (18). We assume that the perturbation vanishes outside some finite interval in the moving frame, that is,

$$V(\tau,t) = 0 \text{ for } |\tau| \geq L \text{ for some } L > 0. \tag{25}$$

Upon substituting (24) into (23) we obtain the linearised perturbation problem and now seek solutions of the form

$$V(\tau,t) = \nu(\tau)e^{-\lambda t}, \tag{26}$$

to obtain an eigenvalue problem for $\nu(\tau)$, where λ is interpreted as an eigenvalue. The equation for ν is then

$$\begin{aligned}\frac{d^2\nu}{d\tau^2} + c\frac{d\nu}{d\tau} + \nu\Bigg\{\lambda + \frac{720b}{\pi^4} - \frac{45}{\pi^2} - \frac{60b}{\pi^2} + \frac{630}{\pi^4} \\ + 2u\left(-\frac{720b}{\pi^5} + \frac{105}{\pi^3} + \frac{60b}{\pi^3} - \frac{1575}{\pi^5}\right) \\ + 3u^2\left(-\frac{70}{\pi^4} + \frac{1050}{\pi^6}\right)\Bigg\} = 0.\end{aligned} \tag{27}$$

The consequent boundary condition on ν due to (25) is

$$\nu(-L) = \nu(L) = 0. \tag{28}$$

To solve our eigenvalue problem (27) and (28) we use the Liouville–Green transformation $\nu = w\exp(c\tau/2)$ to reduce the problem to a Sturm–Liouville problem in w, given by

$$\frac{d^2w}{d\tau^2} + w[\lambda - q(\tau)] = 0, \qquad w(-L) = w(L) = 0, \tag{29}$$

where

$$\begin{aligned}q(\tau) = \frac{c^2}{4} - \frac{720b}{\pi^4} + \frac{45}{\pi^2} + \frac{60b}{\pi^2} - \frac{630}{\pi^4} \\ - 2u\left(-\frac{720b}{\pi^5} + \frac{105}{\pi^3} + \frac{60b}{\pi^3} - \frac{1575}{\pi^5}\right) \\ - 3u^2\left(-\frac{70}{\pi^4} + \frac{1050}{\pi^6}\right).\end{aligned} \tag{30}$$

It is well-known that if $q(\tau) > 0$ and is continuous then the eigenvalues for the problem (29) on the interval $|z| \leq L$ are all positive [13]. Consequently, the problem expressed by equations (27) and (28) has positive eigenvalues if $q(\tau) > 0$, which implies that the wavefront solution $u(\tau)$ given by Eq. (20) is linearly stable, by (26).

From the plots in Figure 5 it is seen that q_1 is always strictly positive. This implies that for the TWS between the second and third roots we will always have positive eigenvalues and hence this particular TWS is linearly stable to small perturbations. However, at this stage, nothing can be concluded about the stability of the remaining two travelling wave solutions since we cannot gaurantee stability because $q(\tau)$ is not strictly positive for $-L \leq \tau \leq L$.

Stability Analysis via a Hardy-Type Inequality

The above stability analysis requires $q(\tau) > 0$ in order to guarantee stability, a condition that is only met for the solution q_1. To extend this stability result we will apply a Hardy-type inequality, as has been deployed in [2,3].

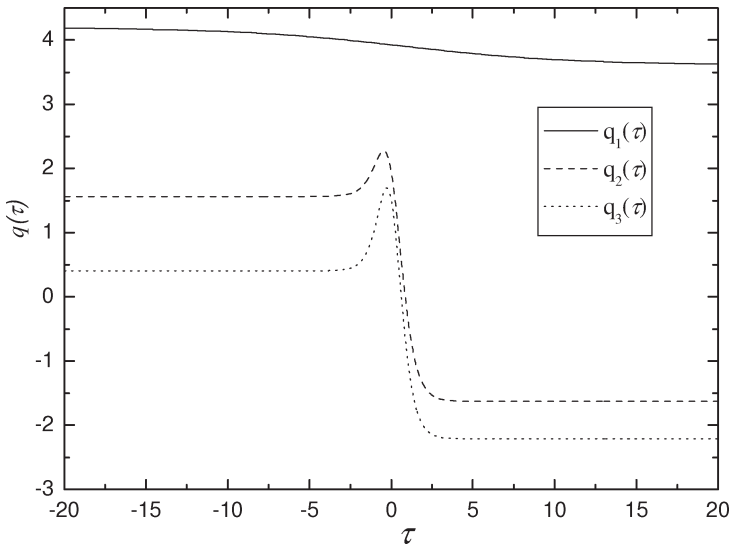

FIGURE 5 Qualitative behaviour of $q(\tau)$ in (30) for the possible TWS in (18) for the roots identified in the text and $b = 0.9$. $q_1(\tau)$ represents $q(\tau)$ for the TWS which travels from u_2 to u_3 as $\tau \to \infty$. Similarly $q_2(\tau)$ and $q_3(\tau)$ represent $q(\tau)$ for the TWS which travel from u_1 to u_2 and u_3 to u_1, respectively.

From (29), our Sturm–Liouville eigenvalue problem may be multiplied throughout by w and integrated to find

$$\lambda \int_{-L}^{L} w^2 d\tau = \int_{-L}^{L} \left[-\frac{d^2 w}{d\tau^2} w + q w^2 \right] d\tau. \tag{31}$$

Integrating by parts and applying the boundary conditions gives

$$\lambda \int_{-L}^{L} w^2 d\tau = \int_{-L}^{L} \left[\left(\frac{dw}{d\tau} \right)^2 + q w^2 \right] d\tau \equiv J(w), \tag{32}$$

where we have introduced the quantity $J(w)$ for convenience. An application of Hardy's inequality [5, p. 105] shows that

$$J(w) \geq \frac{1}{4} \int_{-L}^{L} \left[\frac{w^2}{m^2} + 4 q w^2 \right] d\tau, \tag{33}$$

where $m = \min\{z + L, L - z\}$. Therefore we have

$$\lambda \int w^2 d\tau \geq \frac{1}{4} \int_{-L}^{L} \frac{w^2}{m^2} (1 + 4 q m^2) d\tau. \tag{34}$$

We require $J(w) \geq 0$ for non-negative eigenvalues. Therefore if we can show

$$1 + 4 q m^2 \geq 0, \tag{35}$$

then we can always gaurantee non-negative eigenvalues. However, it can be shown that this condition does not always hold. Nevertheless, through investigations we can see that for relatively small L we always have stability in all cases. Our condition for stability will then be dependent upon L.

It is clear that for all three solutions $1 + 4 m^2 q \geq 1 + 4 L^2 \underline{q}$ where

$$\underline{q} = \min_{-L \leq \tau \leq L} q_3(\tau). \tag{36}$$

Thus, from the requirement (35), we can conclude that

$$1 + 4 L^2 \underline{q} \geq 0 \qquad \text{whenever} \qquad L \leq \sqrt{-1/4\underline{q}} \equiv L_c. \tag{37}$$

Therefore if $|\tau| \leq L_c$ then we can gaurantee stability in all cases. From numerical calculations, $L_c \approx 0.3317$ m. This is a feasible restriction on the length as we would always be dealing with relatively small widths of our samples.

Stability via Lowest Eigenvalue

In many applications involving the stability of liquid crystal deformations the most important piece of information is the lowest eigenvalue λ_1. Equation (29) is the Euler equation corresponding to the problem of finding the extremum of the quadratic functional $J(w)$ introduced at Eq. (32) subject to the boundary conditions $w(-L) = w(L) = 0$. The eigenfunctions can be normalised via the subsidiary condition

$$\int_{-L}^{L} w^2 d\tau = 1, \tag{38}$$

which, as detailed below, then means that the minimum of $J(w)$ corresponds exactly to λ_1. The method we follow will allow us to find an accurate approximation to the first eigenvalue λ_1 with the added bonus of finding a good approximation to the corresponding first eigenfunction. This is a special case of a minimisation problem with an isoperimetric constraint and we shall proceed by initiating the Ritz method following Gelfand and Fomin [6]. We set y_n to be a linear combination of sinusoidal terms satisfying the boundary conditions, namely,

$$y_n = \sum_{k=1}^{n} \alpha_k \sin(k\pi\tau/L). \tag{39}$$

We then proceed to minimise the functional $J(w)$ over the arbitrary constants $\alpha_k,\ k = 1, 2, \ldots, n$, subject to the constraint (38) in terms of y_n, which becomes

$$L \sum_{k=1}^{n} \alpha_k^2 = 1. \tag{40}$$

This is accomplished by minimising the real variable function $J(y_n) - \lambda\left(\int_{-L}^{L} y_n^2\, d\tau - 1\right)$ with respect to the α_k. This leads to the n requirements

$$\frac{\partial}{\partial \alpha_r}\left[J(y_n) - \lambda\left(L \sum_{k=1}^{n} \alpha_k^2 - 1\right)\right] = 0. \tag{41}$$

We then have $n + 1$ equations in the $n + 1$ unknowns α_k and λ provided by the solutions to (40) and (41). Solving these simultaneous equations results in an approximate evaluation of λ_1 by λ (which corresponds to the minimum value of $J(y_n)$) and the corresponding approximate eigensolution y_n. It is known that λ approaches λ_1 monotonically from above as $n \to \infty$.

From MAPLE and MATLAB we can evaluate the above approximation to the lowest eigenvalue for our system. We specialise to the specific case of the material SCE3 with the following material parameters [15]:

$$\epsilon_0 = 8.854 \times 10^{-12}\,\mathrm{F\,m^{-1}}, \qquad \epsilon_a = -1.94, \qquad \lambda_5 = 0.025\,\mathrm{Pas}\,,$$

$$\theta = 9.65^{\mathrm{o}}, \qquad P_0 = 88 \times 10^{-6}\,\mathrm{C\,m^{-2}}.$$

The results are shown in Figure 6.

From our evaluation of λ_1 we may now deduce the response times for such perturbations, expecting them to be of the same order of magnitude as response times for smectic C* liquid crystals. The response times t_r are defined in the usual way [15] via (26) and can be expressed in the original time scale by

$$t_r = \frac{2\lambda_5}{\epsilon_0|\epsilon_a|\sin^2\theta E_0^2}\frac{1}{\lambda_1}. \tag{42}$$

The dependence of t_r upon the electric field and first eigenvalue can be seen in Figure 7.

The response times of the perturbations decrease as the field is increased and appear to be of the same order as those known for SmC* liquid crystals [15]. We may also note that the decay of the

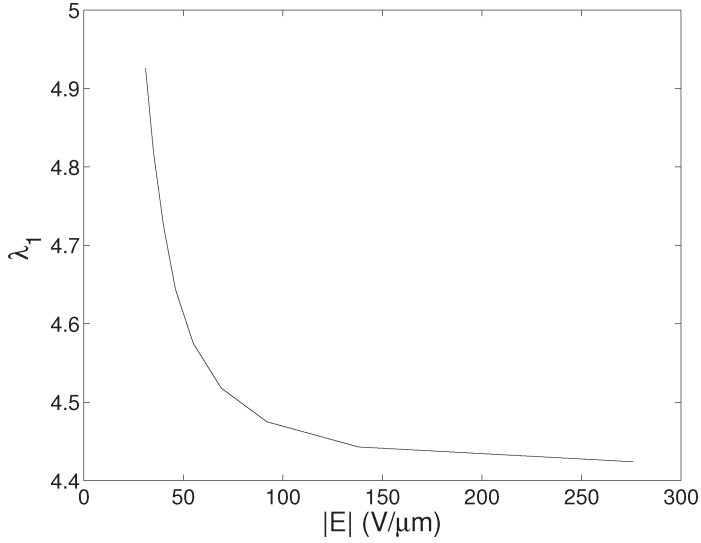

FIGURE 6 Plots of how the first eigenvalue depends upon the electric field.

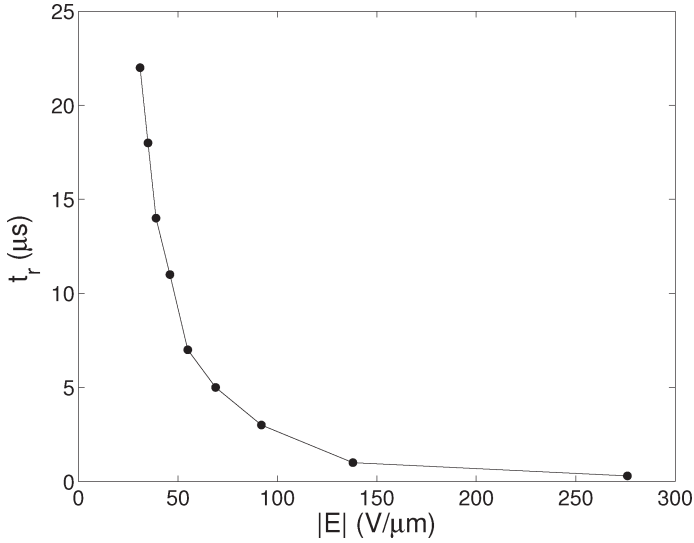

FIGURE 7 The electric field dependence of the perturbation response time t_r.

perturbation is faster than the travelling wave speed and that it does not depend upon the spontaneous polarisation P_0. This response time is for relatively high fields where the polarisation is negligible in comparison. In a low field the spontaneous polarisation is known to be the dominant factor, in which case the form of our response time changes as discussed by Stewart [15, p. 316].

CONCLUSIONS

We have modelled ring patterns in SmC* to include the dielectric term and all radially dependent terms and obtained a dynamic equation which governs the behaviour of such ring patterns given $|b| \leq 1$ and the angular velocity is less than a critical value. These ring patterns have been shown to have a soliton-like behaviour.

We identified a general stability criterion, namely, that $q(\tau)$, defined by (30), be strictly positive. Not all solutions fulfil this condition. Nevertheless, a stability criterion involving a Hardy-type inequality ensured non-negative eigenvalues which therefore guaranteed stability. This is true for all radial distances for q_1, as identified above, while for q_2 and q_3 a restriction on the radial distance $|\tau| \leq L_c$, defined in (37), is necessary to ensure stability. The lowest eigenvalue was determined via an isoperimetric minimisation problem

and the Ritz method. From this we deduced response times for perturbations to the solutions of the model for ring patterns in SmC^* liquid crystals.

REFERENCES

[1] Abramowitz, M. & Stegun, I. A. (1972). *Handbook of Mathematical Functions*, Dover: New York.

[2] Anderson, D. A. & Stewart, I. W. (2001). Stability of non-constant equilibrium states in a finite sample of ferroelectric liquid crystal. *Int. J. Eng. Sci.*, *39*, 1191–1215.

[3] Atkin, R. J. & Stewart, I. W. (2002). Stability of domain walls in cylindrical layers of smectic C liquid crystals. *Q. Jl. Mech. Appl. Math.*, *55*(2), 163–177.

[4] Dascalu, C., Hauck, G., Koswig, H. D., & Labes, U. (1996). Spontaneously created ring structures in free-standing liquid crystal films and their dependence on temperature and material parameters. *Liq. Cryst.*, *21*, 733–743.

[5] Davies, E. B. (1995). *Spectral Theory and Differential Operators*, Cambridge University Press: Cambridge.

[6] Gelfand, I. M. & Fomin, S. V. (1963). *Calculus of Variations*, Dover: New York.

[7] Hauck, G., Koswig, H. D., & Labes, U. (1993). Electric field induced structure formation in free standing ferroelectric films. *Liq. Cryst.*, *14*, 991–997.

[8] Hochstadt, H. (1986). *The Functions of Mathematical Physics*, Dover: New York.

[9] Kilian, A., Koswig, H. D., & Sonnet, A. (1995). Theory of pattern formation in a free-standing ferroelectric film in a rotating electric field. *Mol. Cryst. Liq. Cryst.*, *265*, 321–334.

[10] Lam, L. & Prost, J. (1992). *Solitons in Liquid Crystals*, Springer-Verlag.

[11] Leslie, F. M., Stewart, I. W., & Nakagawa, M. (1991). A continuum theory for smectic C liquid crystals. *Mol. Cryst. Liq. Cryst.*, *198*, 443–454.

[12] Link, R. D., Radzihovsky, L., Natale, G., Maclennan, J., Clark, N. A., Walsh, M., Keast, S. & Neubert, M. (2000). Ring-pattern dynamics in smectic-C^* and smectic-C^*_A freely suspended liquid crystal films. *Phy. Rev. Lett.*, *84*, 5772–5775.

[13] Logan, J. D. (1994). *An Introduction to Nonlinear Partial Diffential Equations*, Wiley: New York.

[14] Oseen, C. W. (1933). The theory of liquid crystals. *Trans. Faraday Soc.*, *29*, 883–899.

[15] Stewart, I. W. (2004). *The Static and Dynamic Continuum Theory of Liquid Crystals*, Taylor & Francis: London & New York.

[16] Zwetkoff, V. (1939). Bewegung anisotroper flussigkeiten im rotierenden magnetfeld. *Acta Physiochimica*, URSS, *10*, 555–578.